Recombination of argon in an expanding plasma jet

M. C. M. van de Sanden, J. M. de Regt, and D. C. Schram
Department of Physics, University of Technology Eindhoven, P.O. Box 513, 5600 MB Eindhoven, The Netherlands
(Received 29 September 1992)

This paper deals with the behavior of an electron gas in an expanding plasma jet in argon. From the measurements, obtained using a high-quality Thomson-Rayleigh scattering diagnostic, it is shown that the collisional-radiative recombination of argon is small. However, the three-particle recombination plays a determining role in the heating of the electron gas. From the relation between the electron density and the electron temperature in the first part of the expansion, the three-particle recombination coefficient is calculated, which shows good agreement with previous results reported in the literature.

PACS number(s): 52.25.Fi, 52.25.Jm, 52.20.Fs, 52.25.Rv

INTRODUCTION

Expanding plasmas are interesting from a fundamental as well as from a technological point of view. Nowadays expanding plasmas are used in plasma processing, e.g., plasma deposition [1,2], plasma sources [3], and recombination lasers. The fundamental interest in expanding plasmas is the different behavior of the electrons and heavy particles during expansion, due to their large mass difference. As a consequence, if the expansion is strong, charge separation can occur, which leads to a generated electromagnetic field [4]. This electromagnetic field in turn influences the behavior of the charged particles in the expanding plasma. Another interesting feature in free expanding plasmas is the coupling between the ionization-recombination phenomena and the flow properties as electron temperature and electron density. In this respect the study of the equilibrium departure is essential, as it can help in the understanding of the kinetic processes involved.

The aim of this paper is to determine the recombination behavior of a freely expanding plasma jet in pure argon. This is achieved by analyzing the measured electron density and temperature and the neutral-particle density, which are obtained from a high-performance Thomson-Rayleigh scattering diagnostic [5,6].

EXPERIMENT

The measurements discussed in this paper are performed on a plasma which expands freely from a subatmospheric-pressure thermal plasma in argon (a cascaded arc, typical values for the temperature $T \approx 1$ eV, the electron density $n_e \approx 10^{22}$ m^{-3}, and the neutral-particle density $n_0 \approx 10^{23}$ m^{-3}) into a low-background-pressure ($p \approx 10-100$ Pa) region [1,2,5,6]. The electron density and temperature and the neutral-particle density in the expansion part are measured locally by means of Thomson and Rayleigh scattering. The main components of the scattering diagnostic are a frequency-doubled Nd:YAG laser (where YAG denotes yttrium aluminum garnet), a polychromator based on a holographic concave grating, and a gateable light amplifier in combination with a linear photodiode array. Much attention is given to the suppression of stray light which is essential if one wants to measure Rayleigh and Thomson scattering simultaneously (the equivalent stray light level corresponds to 0.4-Pa argon at 300 K). One of the main advantages of Thomson-Rayleigh scattering is that the spatially resolved values of n_e, T_e, and n_0 are measured, i.e., no Abel inversion has to be performed. For more details concerning the Thomson-Rayleigh scattering diagnostic, the reader is referred to the original publication [5].

In Fig. 1 a typical example is given of measurements of n_e, T_e and n_0 on the axis of the plasma jet. The conditions of the plasma are indicated in the figure caption. The strong supersonic expansion (about three orders of magnitude) can be clearly seen. After several centimeters (the position of the shock depends on the background pressure), a shock occurs. After the shock the plasma expands further subsonically. The position of the jump in the electron temperature occurs before the jump in the densities. The difference is due to the electrical currents generated in the first part of the expansion. Similar measurements were discussed by Fraser, Robben, and Talbot [7] and Poissant and Dudeck [8]. In this paper we will concentrate on the behavior of the densities and the electron temperature in the first region, i.e., until the jump in the electron temperature occurs.

ANALYSIS

In Fig. 2 the measured electron and neutral-particle densities in the first part of the expansion corresponding with Fig. 1 are compared with the model of Ashkenas and Sherman [9]. This model was originally developed for the adiabatic supersonic expansion of ideal gases. Following this model the densities scale as

$$n = \frac{n_{\mathrm{res}} z_{\mathrm{ref}}^2}{(z - z_0)^2} , \tag{1}$$

for $z \gg z_0$. Equation (1) is the well-known source expansion with n_{res} the reservoir particle density, z_0 the origin from which the particle trajectories seem to originate, and z_{ref} a reference length. As can be seen from Fig. 2 the agreement of Eq. (1) with the measurements of n_0 and

n_e is excellent. The interpretation of Eq. (1) is as follows. During the expansion thermal energy is converted adiabatically into directed kinetic energy. Since the thermal energy is limited by the total enthalpy in the reservoir (in the present case the condition at the end of the cascaded arc), the velocity $w_{\rm axis}$ along the axis saturates and becomes finally constant. From flux conservation this means that for a source expansion of the product $nw_{\rm axis}A = \text{const}$. Since the area A of the plasma jet scales as z^2, the densities scale as z^{-2} for large z [cf. Eq. (1)]. For a plasma, however, Eq. (1) is only valid if the recombination or ionization can be neglected compared with the change of density due to the expansion. In Table I the parameters z_0 and $n_{\rm res}$, corresponding to the different settings of Table II are given. As can be seen from Table I, for the same settings of the plasma, the parameters z_0 and $n_{\rm res}$ for the electron and neutral-particle density are the same within the estimated error. This means that the change of the ionization degree during expansion of the plasma is minimal. Another conclusion is that for the same *arc* settings but different vessel pressure the fitting parameters are equal, indicating the supersonic nature of the expansion. Hence from Table I it can be concluded that the recombination of argon during the expansion is much smaller than the decrease of the densities due to the expansion of the plasma. Smaller in this sense of course also means a smaller loss of ionization than can be measured with enough accuracy with the Thomson-Rayleigh scattering diagnostic.

In this paper we shall use an alternative approach to determine the recombination of argon in an expanding plasma jet by means of the electron energy balance. In Fig. 3 n_e as a function of T_e is shown in the expansion for

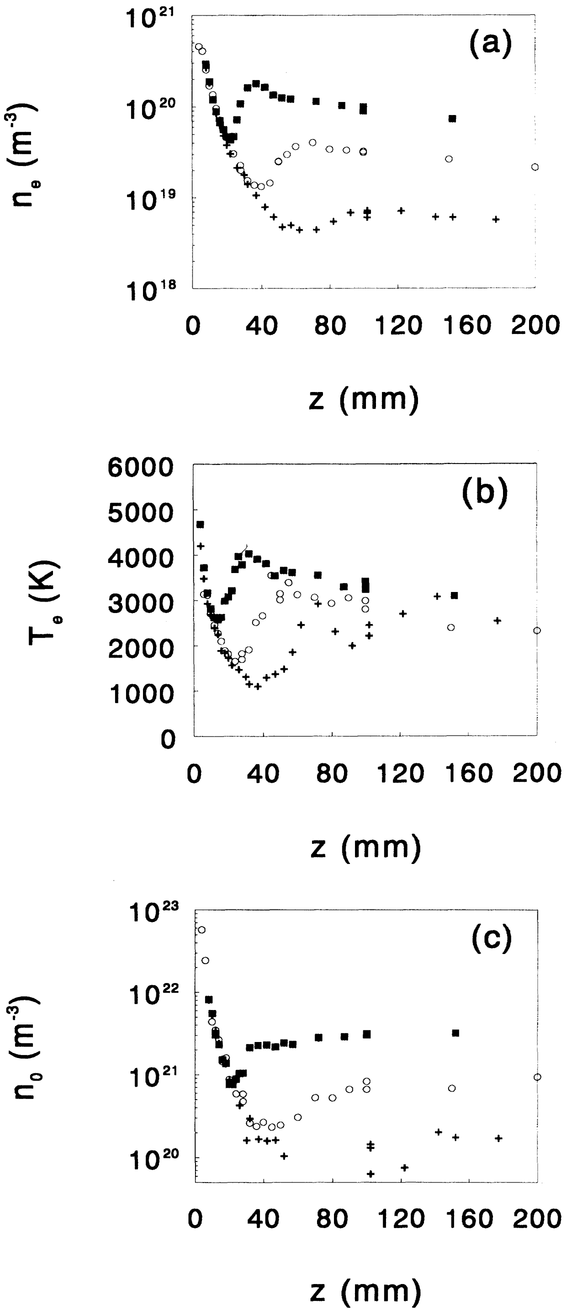

FIG. 1. (a) n_e (b) T_e, and (c) n_0 on the axis as a function of the axial position for different background pressures. $I_{\rm arc} = 45$ A; the Ar flow is 58 SCCS (cubic centimeter per second at standard temperature and pressure); +, 13.3 Pa; ○, 40 Pa; ■, 133 Pa.

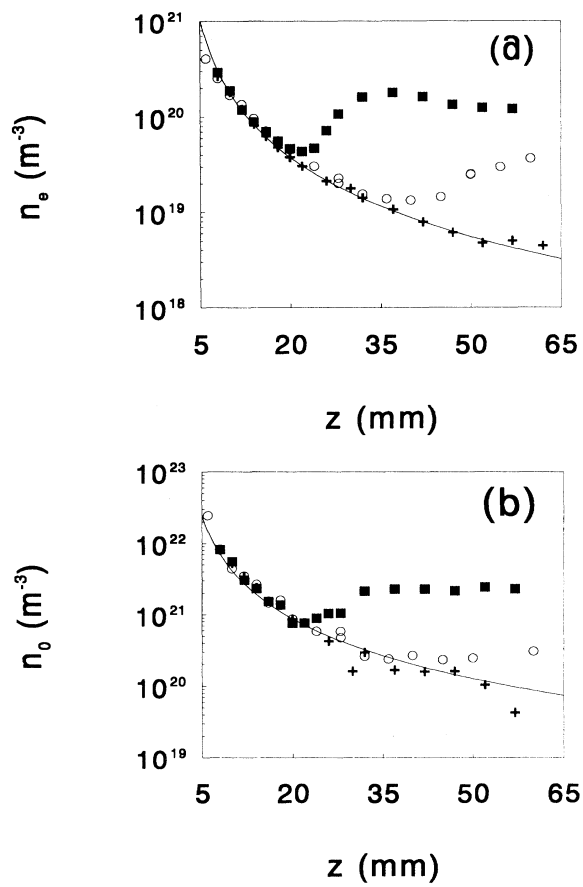

FIG. 2. n_e and n_0 on the axis as a function of the axial position for different background pressures compared with the model of Ashkenas and Sherman (lines) [9]. $I_{\rm arc} = 45$ A; the Ar flow is 58 SCCS; +, 13.3 Pa; ○, 40 Pa; ■ 133 Pa.

TABLE I. The fitting parameters z_0 and $n_{\rm res}$ for the electron and the neutral-particle density in the expansion.

Settings	$z_{0,e}$ (mm)	$n_{{\rm res},e}$ (10^{22} m^{-3})	$z_{0,0}$ (mm)	$n_{{\rm res},0}$ (10^{23} m^{-3})
1	1.5±0.5	1.3±0.3	1.5±0.5	3.0±0.3
2	1.5±0.5	1.3±0.3	1.5±0.5	3.0±0.3
3	1.5±0.5	1.3±0.3	1.5±0.5	3.0±0.3
4	2.5±0.5	1.5±0.3	2.5±0.5	3.0±0.3
5	3.5±0.5	1.7±0.3	3.5±0.5	2.0±0.3

the plasma settings as given in Table II. As can be seen a simple scaling law is found which reads

$$T_e^{\chi}=C_0 n_e \ . \tag{2}$$

The parameters χ and C_0 can be determined from a weighted least-mean-squares analysis and are equal to $\chi=3.47\pm0.26$ and $C_0=4.7\times10^{-9}$ m^3 K$^{3.47}$. The accuracy in C_0 is approximately a factor 3. A result similar to Eq. (2) was found by Stevefelt and Collins [12] from a numerical model for a laser-produced carbon plasma. The explanation is the fact that, although the three-particle recombination can be neglected in discussing the behavior of the electron density in the expansion, it can*not* be neglected on the energy scale, i.e., it has to be taken into account as a heat source for the electron gas. Therefore the electron gas does not expand adiabatically (corresponding with $\chi=\frac{3}{2}$). Here we will use a simple quasi-one-dimensional model [2] to demonstrate that the result Eq. (2) is indeed due to three-particle recombination. Moreover, as we shall see, the result Eq. (2) gives a means to determine the three-particle recombination rate $K_{{\rm rec},3}$.

The equations we need are the time-dependent mass and energy balance for the electron gas,

$$\nabla\cdot n_e \mathbf{w}_e=0 \ , \tag{3}$$

$$\nabla\cdot(\tfrac{3}{2}n_e k_b T_e \mathbf{w}_e)+n_e k_b T_e \nabla\cdot\mathbf{w}_e=Q_e \ . \tag{4}$$

Here $\mathbf{w}_e$ is the electron flow velocity and Q_e are the heat and loss sources for the electron gas. In Eq. (3) we used the fact that the loss of ionization in the mass balance can be neglected. The main ion in the expansion is assumed to be the Ar^+ ion. The Ar_2^+ ion is suspected to be present, although in small quantities ($n_{Ar^+}/n_{Ar_2^+}\approx10^{-5}$). Therefore the molecular ion is totally omitted in the present analysis. In Eq. (6) electron heat conduction is also neglected. The ratio between the electron heat conduction term and the transport term in Eq. (4) is approximately

$$\frac{v_{\rm thermal}\lambda_{ee}L_{n_e}}{w_e L_{T_e}^2} \ . \tag{5}$$

In Eq. (5) $v_{\rm thermal}$ is the thermal velocity of the electrons, λ_{ee} the mean free path for electron-electron collisions, and L_{T_e} and L_{n_e} are typical gradient lengths in the expansion for the temperature and density, respectively. Typical values in the expansion for $T_e=2000$ K are $v_{\rm thermal}=5\times10^5$ m/s, $w_e=3\times10^3$ m/s, $\lambda_{ee}=5\times10^{-5}$ m, $L_{n_e}=10^{-2}$ m, and $L_{T_e}=L_{n_e}\times3.47=3.47\times10^{-2}$ m. This gives for the ratio [cf. Eq. (5)] 0.07 so that heat conduction can be neglected [2]. Furthermore the Joule dissipation by pressure-induced electrical currents [4,5,6] is also omitted in Eq. (4). For the same reason, i.e., since $\lambda_{ee}\ll L$, and since the expansion is supersonic the effect of ambipolar diffusion is minimal on the results presented. The main assumption of the present analysis therefore will be the structure of Q_e. We assume that Q_e can be written as

$$Q_e=Q_{{\rm rec},3}=K_{{\rm rec},3}E_{{\rm rec},3}n_e^3=C_{{\rm rec},3}E_{{\rm rec},3}n_e^3T_e^{\beta} \ , \tag{6}$$

i.e., the electron gas is mainly heated by three-particle recombination. In Eq. (6) $C_{{\rm rec},3}$ and β are constants and

TABLE II. The different settings of the cascaded-arc setup. For explanation see text. The flow is given in units of cm^3/s at standard pressure and temperature (SCCS).

Settings	$I_{\rm arc}$ (A)	Ar flow (SCCS)	p (Pa)
1	45	58	40
2	45	58	13.3
3	45	58	133
4	45	75	40
5	60	58	40

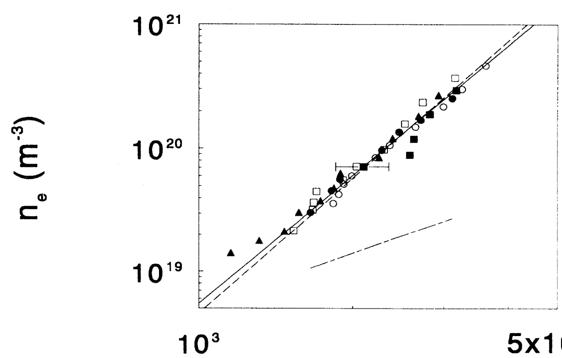

FIG. 3. n_e as a function of T_e in the expansion for different settings of the cascaded arc and different background pressures (cf. Table II): (1) ●, (2) ■, (3) △, (4) □, and (5) ○. The different lines indicate the following: ——, slope 3.47±0.26; – – – –, slope $\frac{11}{3}$, and — — —, slope $\frac{3}{2}$.

$E_{\rm rec,3}$ is the mean recombination energy which is released in the recombination reaction

$$\mathbf{e}+\mathbf{e}+\mathbf{A}^{+}\rightarrow\mathbf{e}+\mathbf{A}_{p} \ . \tag{7}$$

$E_{\rm rec,3}$ in general depends on the collisional-radiative behavior of the plasma concerned, and should follow a collisional-radiative model such as can be found, for example, in Ref. [13]. Here we will use a simplified approach in the determination of $E_{\rm rec,3}$. Note that we assume that $K_{\rm rec,3}$ is only a function of T_e [cf. Eq. (6)]. A value commonly found for the exponent β is $-\frac{9}{2}$ [10,11,13–15], which also follows from the simple Thomson theory [10,14].

Using the quasi-one-dimensional approach [2] Eqs. (3) and (4) are rewritten

$$A^{-1}\frac{d(n_e w_{eA} A)}{dz}=0 \ , \tag{8}$$

$$\tfrac{3}{2}n_e w_{eA} k_b \frac{dT_e}{dz}-k_b T_e w_{eA}\frac{dn_e}{dz}=C_{\rm rec,3}E_{\rm rec,3}n_e^3 T_e^{\beta} \ , \tag{9}$$

where w_{eA} is the drift velocity normal to the area A of the plasma jet at the axial position z. The solution of Eq. (8) is given by Eq. (1). Substitution of Eq. (2) in Eq. (9) leads to a single differential equation for T_e,

$$(\tfrac{3}{2}-\chi)w_{eA}k_b\frac{dT_e}{dz}=C_{\rm rec,3}E_{\rm rec,3}C_0^{-2}T_e^{2\chi+\beta} \ . \tag{10}$$

Note that $\chi=\frac{3}{2}$ is excluded as is apparent from Eqs. (9) and (10). The solution of Eq. (10) is

$$T_e=\left[(-2\chi-\beta+1)\frac{C_{\rm rec,3}E_{\rm rec,3}}{(\frac{3}{2}-\chi)C_0^2 w_{eA}k_b}\right]^{(-2\chi-\beta+1)^{-1}} \times(z-z_0)^{(-2\chi-\beta+1)^{-1}} \ . \tag{11}$$

Combining Eqs. (1), (2), and (11) leads to two algebraic relations for β and $C_{\rm rec,3}$.

$$\beta=1-\tfrac{3}{2}\chi \ , \tag{12}$$

$$C_{\rm rec,3}=\frac{C_0^2 w_{eA}k_b(\frac{3}{2}-\chi)}{E_{\rm rec,3}(-2\chi-\beta+1)}(C_0 n_{\rm res,e}z_{\rm ref}^2)^{(-2\chi-\beta+1/\chi)} . \tag{13}$$

Now two routes to determine $K_{\rm rec,3}$ can be followed (cf. Table III). If we use the commonly accepted value of $\beta=-\frac{9}{2}$, the exponent χ becomes [cf. Eq. (12)] $\chi=\frac{11}{3}$. This value of χ gives a good representation of the measured data as can be seen in Fig. 3, where a line with this slope is indicated. Furthermore, the value of $\chi=\frac{11}{3}$ is in agreement with the determined weighted least-mean-squares value of $\chi=3.47\pm0.26$. For the value of $\chi=\frac{11}{3}$, the value of C_0 is determined with a higher accuracy. The value found in $C_0=2.2\times10^{-8}$ m^3 K$^{11/3}$ with an accuracy of a factor 1.3. To determine the absolute value of $C_{\rm res,3}$ we have to know w_{eA} and $E_{\rm rec,3}$. We shall come back to this point later on. The second method is the weighted least-mean-squares result for both χ and C_0. In this case the mentioned $\chi=3.47\pm0.26$ is found and the value for $C_0=4.7\times10^{-9}$ m^3 K$^{3.47}$, with the mentioned accuracy in C_0 of approximately a factor 3. The corresponding value of β is $\beta=-4.20\pm0.39$ in agreement with the commonly found value of $\beta=-\frac{9}{2}$. For both cases the value of $C_{\rm res,3}E_{\rm rec,3}/w_{eA}$, the only unknown from Eq. (13), is given in Table III. In the least-mean-squares analysis we have taken all data of Fig. 3 into account, although $n_{\rm res,e}$ is not equal for all the settings (cf. Table I). However, $C_{\rm rec,3}$ is according to Eq. (13) proportional to $n_{\rm res,e}^{\gamma}$ with $\gamma\approx0.41$ for the two cases. Hence the small differences in $n_{\rm res,e}$ for the different settings lead to small differences in $C_{\rm rec,3}$.

To determine the absolute value of $C_{\rm rec,3}$, we have to know the ratio $E_{\rm rec,3}/w_{eA}$. Since the ratio is of sole importance, we concentrate here on the possible values of $E_{\rm rec,3}$, and fix w_{eA} at a value found in experiments [2], i.e., $w_{eA}=3000$ ms^{-1}. Furthermore, we assume that the recombination energy depends weakly on the electron temperature and can be considered constant for the parameter range of the present analysis. As mentioned the recombination energy $E_{\rm rec,3}$ should follow from a collisional-radiative model for the Ar I system. Here the recombination energy is estimated by comparing the collisional deexcitation with the radiative deexcitation. First, the *effective* 4*s* levels are considered, which are situated at a mean energy of $E_{4s}=11.58$ eV and consist of the four 4*s* levels. According to Rosado [16], the effective transition probability (i.e., averaged over the four 4*s* levels) for the $4s^{\rm eff}$ levels is equal to 10^8 s^{-1}. For $n_e\approx10^{20}$ m^{-3} and $n_0\approx10^{21}$ m^{-3}, it can be shown that the escape factor for $4s^{\rm eff}$ to the ground-state transition is equal to 10^{-2}, i.e., the radiative transitions to the ground state are optically thick. The deexcitation by electron collisions for the same transitions is equal to $10^{20}\times2\times10^{-16}=2\times10^4$ s^{-1}, where we used a deexcitation rate for $4s^{\rm eff}\rightarrow$ ground-state transition of 2×10^{16} m^3 s^{-1} [16]. Comparing the radiative excitation with the collisional deexcitation, it is easily seen that the deexcitation by radiative processes is still dominant for the $4s^{\rm eff}$ levels, even though there is substantial reabsorption. This reasoning remains valid for electron densities up to 10^{21} m^{-3}. This means that the recombination energy is not equal to the ionization energy $I_{\rm ion}$, but is smaller by at least 11.58 eV, because this recombination energy is

TABLE III. The results of the least-mean-squares analysis for the two cases. For explanation see text. The numbers in parentheses are the accuracy factors, i.e., the accuracy is with a factor of 1.3 in C_0 (for 2.2×10^{-8}).

Case	χ	C_0	β	$C_{\rm rec,3}E_{\rm rec,3}/w_{eA}$	$C_{\rm rec,3}$
1	11/3	2.2×10^{-8} (1.3)	$-9/2$	4.6×10^{-43} (3)	3.3×10^{-21} (3)
2	3.47 ± 0.26	4.7×10^{-9} (3)	-4.60 ± 0.39	4.4×10^{-44} (10)	3.2×10^{-22} (10)

lost by radiation. A similar analysis for the $4p^{\text{eff}} \rightarrow 4s^{\text{eff}}$ transitions shows that these transitions are dominated by radiative transitions too if $n_e \approx 10^{20}$ m^{-3} and $n_0 \approx 10^{21}$ m^{-3}. This means that the recombination energy is again lowered by approximately 1.6 eV. The resulting estimate of the recombination energy is approximately $E_{\text{rec},3} \approx 2.6$ eV. Levels higher than $4p^{\text{eff}}$ are dominated by collisional deexcitation, since the deexcitation rates increase for higher levels [10].

Since we know $E_{\text{rec},3}$ we can calculate $C_{\text{rec},3}$ for the two mentioned cases. In Table III $C_{\text{rec},3}$ is given for $E_{\text{rec},3} = 2.6$ eV and $w_{eA} = 3000$ ms^{-1}. For case 1 we find $C_{\text{rec},3} = 3.3 \times 10^{-21}$ m^6 K$^{9/2}$ s^{-1} with an accuracy of a factor 3. This value compares very well with the value for helium found in the literature [10,11,17] which equals $C_{\text{rec},3} = 1.1 \times 10^{-20}$ m^6 K$^{9/2}$ s^{-1}. As indicated in Refs. [10,11], the differences in $C_{\text{rec},3}$ are small for the different elements since the top of the atomic systems all behave hydrogenlike. For case 2 we find $C_{\text{rec},3} = 3.3 \times 10^{22}$ m^6 K$^{4.2}$ s^{-1} with an accuracy of a factor 10. The two cases are also illustrated in Fig. 4. As can be seen the differences between the two determined recombination coefficients are small within the temperature range of interest (1000–5000 K). Note that the accuracies indicated for $C_{\text{rec},3}$ are excluding the (systematic) inaccuracies in the estimated values of $E_{\text{rec},3}$ and w_{eA}. Other methods to determine $K_{\text{rec},3}$ use the change in electron density either in space or time [18–20]. In the present case, however, these methods would fail because n_e does not change significantly due to the three-particle recombination. Here the information about the recombination of argon is obtained using the specific structure of T_e.

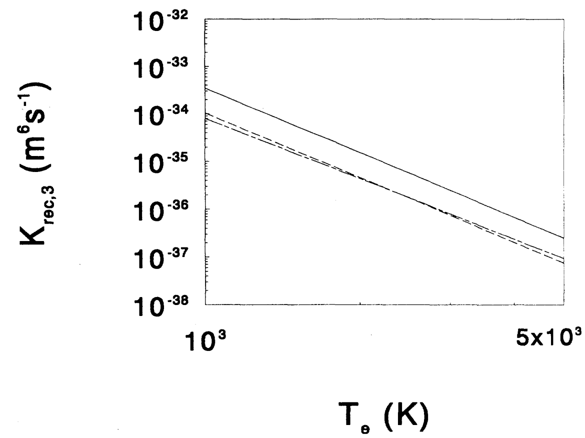

FIG. 4. The experimentally determined recombination coefficient $K_{\text{rec},3}$ as a function of T_e (cf. Table III): ——, Refs. [10,11,17]; ----, case 1; and ———, case 2.

CONCLUSIONS

It is demonstrated that the behavior of the electron and neutral-particle density in the expansion of a freely expanding plasma jet in argon can be described by the model of Ashkenas and Sherman [9], which means that the recombination of argon is small. From the behavior of T_e in connection with the behavior of n_e in the expansion it is concluded that three-particle recombination is the main heat source in the electron energy balance. This means that although three-particle recombination can be neglected in the mass balance, it plays a dominant role as a heat source in the electron energy balance. However, this does not mean that other heat sources do not play a role in the expanding plasma jet in argon. For instance, the observed difference in position between the density shock fronts and the jump in the electron temperature is determined by electric currents induced by the strong pressure gradient [21].

From the analysis of the behavior of the electron gas in the first part of the expansion, the three-particle recombination coefficient $K_{\text{rec},3}$ is determined. The $K_{\text{rec},3}$ found is in agreement with the commonly found $K_{\text{rec},3}$ in the literature showing the $T_e^{-9/2}$ dependence. The absolute value of $K_{\text{rec},3}$ is determined using a simplified model of the collisional-radiative behavior of the plasma studied. From this model an estimate is calculated for the recombination energy which is combination with the least-mean-squares analysis of the n_e-T_e behavior gives an absolute value of $k_{\text{rec},3}$ in agreement with the value from the literature [17].

ACKNOWLEDGMENTS

We would like to thank M. J. F. van de Sande, H. M. M. de Jong, and A. B. M. Hüsken for their skillful technical assistance and J. A. M. van der Mullen for helpful discussions. The research of M. C. M. van de Sanden has been made possible by support from The Royal Netherlands Academy of Arts and Sciences.

[1] J. J. Beulens, A. J. M. Buuron, and D. C. Schram, Surf. Coat. Tech. **47**, 401 (1991).
[2] G. M. W. Kroesen, D. C. Schram, and J. C. M. de Haas, Plasma Chem. Plasma Proc. **10**, 531 (1990).
[3] M. J. de Graaf, R. P. Dahiya, J. L. Jeauberteau, F. J. de Hoog, M. J. F. van de Sande, and D. C. Schram, J. Phys. (Paris) Colloq. **18**, C5-387 (1990).
[4] H. J. G. Gielen and D. C. Schram, IEEE Trans. Plasma Sci. **18**, 127 (1990).
[5] M. C. M. van de Sanden, J. M. de Regt, G. M. Janssen, D. C. Schram, J. A. M. van der Mullen, and B. van der Sijde, Rev. Sci. Instrum. **63**, 3369 (1992).
[6] M. C. M. van de Sanden, Ph. D. thesis, University of Technology of Eindhoven, the Netherlands, 1991.
[7] R. B. Fraser, F. Robben, and L. Talbot, Phys. Fluids **14**, 2317 (1971).
[8] G. Poissant and M. Dudeck, J. Appl. Phys. **58**, 1772 (1985).
[9] H. Ashkenas and F. S. Sherman, in *Rarefied Gas Dynamics,* edited by J. H. de Leeuw (Academic, New York,

1966).
[10] J. A. M. van der Mullen, Phys. Rep. **191**, 109 (1990).
[11] L. M. Biberman, V. S. Vorob'ev, and I. T. Yakubov, *Kinetics of Nonequilibrium Low Temperature Plasmas* (Plenum, New York, 1987).
[12] J. Stevefelt and C. B. Collins, J. Phys. D **24**, 2149 (1991).
[13] D. Benoy, J. A. M. van der Mullen, M. C. M. van de Sanden, B. van der Sijde, and D. C. Schram, J. Quant. Spectrosc. Radiat. Transfer **49**, 129 (1993).
[14] N. D'Angelo, Phys. Rev. **140**, A1488 (1965).
[15] B. Makin and J. C. Keck, Phys. Rev. Lett. **11**, 281 (1963).
[16] R. J. Rosado, Ph. D. thesis, University of Technology of Eindhoven, the Netherlands, 1981.
[17] E. Hinnov and J. G. Hirschberg, Phys. Rev. **125**, 795 (1962).
[18] A. Funahashi and S. Takeda, J. Phys. Soc. Jpn. **25**, 298 (1968).
[19] O. Igra, Prog. Aerospace Sci. **16**, 299 (1975).
[20] A. F. P. Houwing, R. R. Boyce, D. J. Bone, and D. K. Johnston, Shock Waves **1**, 177 (1991).
[21] M. C. M. van de Sanden, J. M. de Regt, and D. C. Schram (to be published).